Chapter 5

Effect of Annealing on the spectral and NLO characteristics of thin films of nano ZnO

Abstract

The annealing effect on the spectral and nonlinear optical characteristics of ZnO thin films deposited on quartz substrates by sol gel process is investigated. As the annealing temperature increases from 300-1050^{0}C, there is a decrease in the bandgap which indicates the changes of the interface of ZnO. Systematic studies on nano crystallites have indicated the presence of luminescence due to excitonic emissions when excited with 255 nm as well as significant contribution from surface defect states when excited with 325 nm. The intensity of UV peak remains the same while the intensity of the visible peak increases with increase in annealing temperature. The mechanism of the luminescence is discussed. Nonlinear optical response of these samples is studied using nanosecond laser pulses at off-resonance wavelengths. The nonlinear absorption coefficient increases from 2.9×10^{-6} m/W to 1.0×10^{-4} m/W when the annealing temperature is increased from 300ºC to 1050 ºC, mainly due to the enhancement of interfacial state and exciton oscillator strength. The third-order optical susceptibility $\chi^{(3)}$ increases with increase in annealing temperature (T) within the range of our investigations. In the weak confinement regime, $T^{2.5}$ dependence of $\chi^{(3)}$ is obtained for ZnO thin films. The role of annealing temperature on the optical limiting response is also studied.

The results of this chapter are published in

Litty Irimpan et.al., "*Effect of annealing on the spectral and nonlinear optical characteristics of thin films of nano ZnO*" Journal of Applied Physics 2008 (In Press)

5.1 Introduction

ZnO as a compound semiconductor has drawn considerable attention for its excellent piezoelectric and optical properties[1] which make it useful to develop the fabrication of integrated acousto-optic devices and ultraviolet photonic devices[2]. Because of its intrinsic thermal stability, ZnO is a good candidate for high temperature optoelectronic devices. ZnO films grown on silicon[3-4], sapphire[4-7], $LiNbO_3$[8], GaAs[9] and quartz[10-12] substrates have been studied and the properties such as photoluminescence[3, 13-14], optical absorption[4,7,10,12] and optical nonlinearities[6,11,15-17] have been investigated. ZnO films have been prepared using various techniques like sol-gel process, laser ablation[4], laser deposition[11], electron beam evaporation[7], molecular-beam epitaxy[6] and sputtering[3,5,9,10,12]. It has been found that the substrate temperature[18], sputtering power[5,19], oxygen partial pressure [5,20] and post-treatments[10,12,21] may significantly influence the structure and optical properties of the films, since the electrical and the optical properties are strongly affected by the interface and the structure of the films. In this chapter, we present the effect of annealing on the spectral and nonlinear optical properties of the ZnO films on quartz substrates annealed within the temperature range of 300-1050ºC.

5.2 Theory

As the temperature increases, the particle size increases due to thermal expansion. Over small temperature ranges, the fractional thermal expansion of uniform linear objects is proportional the temperature change[22]. Different substances expand by different amounts and hence the knowledge of expansion coefficient is necessary to quantify the thermal expansion. The change in temperature determines the fractional change in length and hence the relationship governing the linear expansion of a long thin rod of length L_0 can be written as,

$$\Delta L = L_0 \alpha \Delta T \quad \text{and} \quad L = L_0 \left[1 + \alpha \Delta T\right] \tag{5.1}$$

where, ΔL is the change in length for a temperature change ΔT and α is the linear expansion coefficient. Area expansion is like a photographic enlargement.

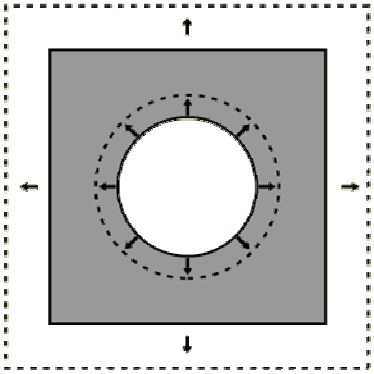

Figure 5.1 Thermal expansion of a material

Thermal expansion of an area, A can be calculated from the linear expansion coefficient.

$$A = L^2 = L_0^2 \left[1 + 2\alpha \Delta T + \alpha^2 \Delta T^2\right] \approx A_0 \left[1 + 2\alpha \Delta T\right] \tag{5.2}$$

and the expanded volume has the form,

$$V = L^3 = L_0^3 \left[1 + 3\alpha \Delta T + 3\alpha^2 \Delta T^2 + \alpha^3 \Delta T^3\right] \approx V_0 \left[1 + 3\alpha \Delta T\right] \tag{5.3}$$

since in most cases the quadratic and cubic terms in the above expression can be neglected because of the fact that the typical expansion coefficient is of the order of parts per million per degree celsius[22]. Every linear dimension increases by the same percentage with a change in temperature, including holes. This assumes that the expanding material is uniform. Thus as the temperature increases, the particle size increases and the size dependent enhancement of exciton oscillator strength is explained in detail in chapter 3.

Optical bandgap reductions with increase in temperature mainly arise from the change of the lattice constant[23]. The temperature dependence of bandgap is given by[24]

$$E_g(T) = E_g - \frac{\alpha\Theta}{2}\left[\sqrt[p]{1+\left(\frac{2T}{\Theta}\right)^p} - 1\right] \qquad (5.4)$$

where α is the slope parameter, Θ is the average phonon temperature and p is the phonon dispersion parameter. Varshini approximation[25] is often employed using empirical parameters A and B is given by

$$E_g(T) = E_g - \frac{AT^2}{B+T} \qquad (5.5)$$

For ZnO, the empirical Varshini parameters A and B are calculated to be 5.05×10^{-4} and 900 respectively[26] upto 300K.

5.3 Synthesis

The ZnO films are deposited on quartz substrates at room temperature by the technique of spin coating. A stable hydrolysed solution is prepared using stoichiometric quantities of zinc acetate dissolved in isopropyl alchohol and the solution is used for spin coating ZnO thin films on quartz substrates by rotating the deposition system at 2000 rotations per minute. The series of samples are then dried at 110°C for half an hour and then placed in a furnace for annealing. The samples are annealed at temperatures of 300^0C, 600ºC, 750ºC, 850ºC, 950ºC and 1050ºC and marked as a-300, b-600, c-750, d-850, e-950, f-1050 respectively. The samples are held at each temperature for three hours in air and then cooled to room temperature slowly with a cooling rate of 0.1^0C per minute.

5.4 Absorption spectroscopy

Figure 5.2 gives the room temperature absorption spectra of the ZnO thin films. When the samples are held at each temperature for a short duration of less than one hour, there is no change in the absorption spectrum

since the temperature driven aggregation regains its original size with slow cooling. But when the samples are held at each temperature for a long duration of much greater than one hour followed by slow cooling, there exist an irreversible change in particle size which increases with increase in annealing temperature. The excitonic peak is found to be blue shifted (370-350 nm) with decrease in particle size with respect to that of bulk ZnO and this could be attributed to the confinement effects[27].

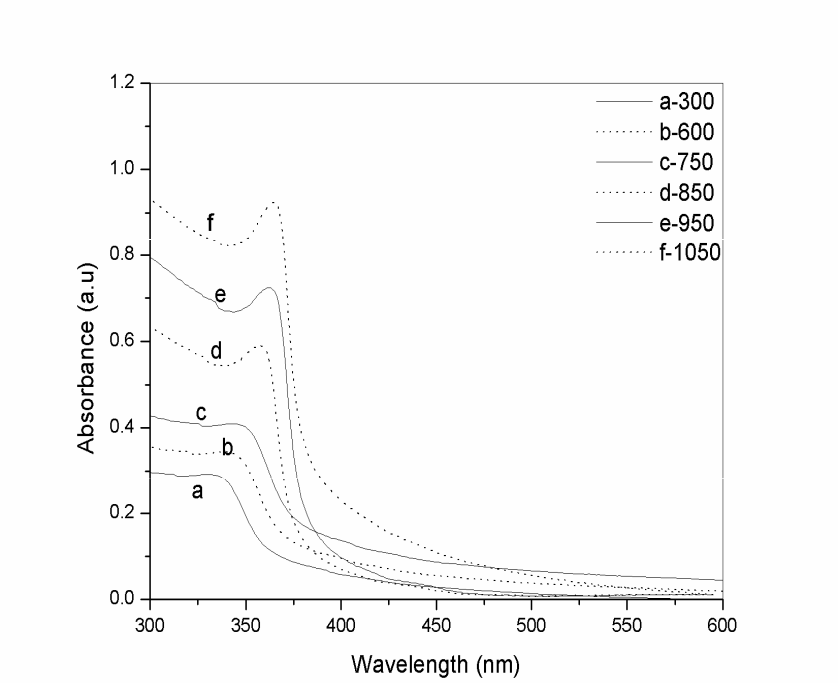

Figure 5.2: Absorption spectra of the ZnO thin films on quartz substrate at different annealing temperatures

By the quantum size effect in nanosized semiconductors, the bandgap increases when the size of the particle is decreased, resulting in a blueshift of the absorption bands. An order of magnitude estimate of the

particle size is possible from the absorption spectra and it is calculated as described in chapter 2.

The ZnO crystallite size increases exponentially from about 4 nm to 85 nm with the rise of the annealing temperature from 300 to 1050 ºC as shown in figure 5.3. The quadratic term in equation 5.3 cannot be neglected since the thermal expansion coefficient[28] of ZnO is of the order of $7x10^{-6}K^{-1}$ and hence we get a nonlinear change in particle size with annealing temperature. In ZnO, the exciton Bohr radius is 2 nm and hence the average particle size of ZnO thin films comes under weak confinement[29] regime ($R>a_B$).

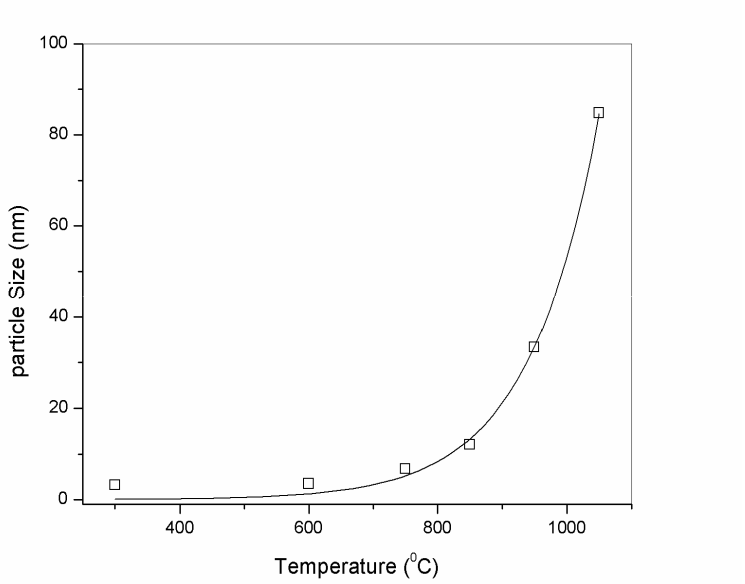

Figure 5.3: Variation of particle size as a function of annealing temperature for ZnO thin films

5.5 Optical bandgap

The direct bandgap is estimated from absorption spectrum as described in chapter 2. The absorption peak of the films shifted towards

lower energy at a higher annealing temperature. The optical bandgap (E_g) is found to be temperature dependent and there is a decrease in the bandgap of the semiconductor with increase in the annealing temperature as shown in figure 5.4. As the films are annealed at a higher temperature the crystallites began to move and tend to agglomerate easily. As a result, the bandgaps of the nanocomposites decrease with increasing annealing temperature.

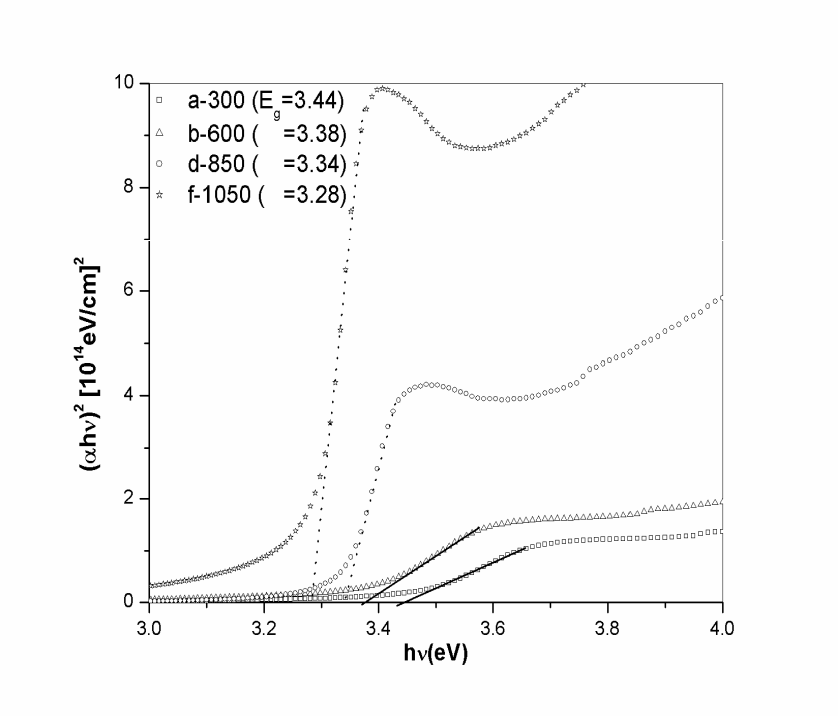

Figure 5.4: Optical bandgap of ZnO thin films at different annealing temperatures. Value of optical bandgap is given in the bracket in the inset legend

The shift of bandgap energy is related to the structural property. Since ZnO thin film has a tensile built-in strain, it can be relaxed by providing sufficient thermal energy. If the tensile strain is relaxed, the bandgap energy is decreased. The bandgap is found to vary in the range 3.28-

3.44 eV in the range of annealing temperatures from 300-1050ºC and is in agreement with the reported value[30].

5.6 Fluorescence spectroscopy

The fluorescence spectra of nano ZnO colloids of different particle size for an excitation wavelength of 255 nm are shown in figure 5.5. Figure shows multiple emission peaks at 390 nm, 420 nm, 490 nm and 530 nm. Additional shoulders at 455 nm, 570 nm and 600 nm are present along with the emission peaks. These may be attributed to transition from various excited state energy levels of exciton to the ground level corresponding to $R>>a_B$ case and the series of peaks can be modelled as a particle in a box problem as described in chapter 2.

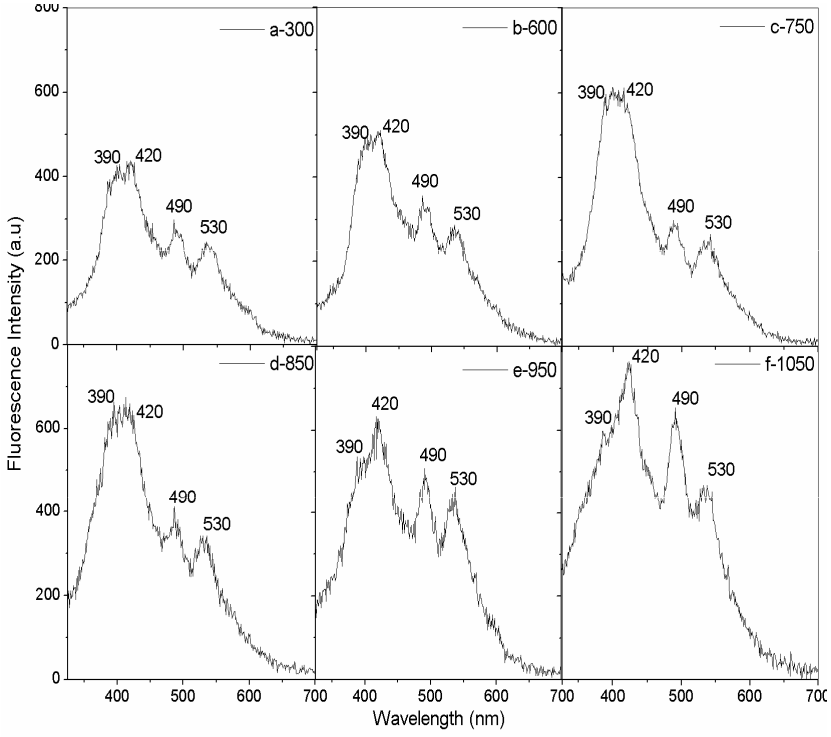

Figure 5.5: Fluorescence spectra of ZnO thin films at different annealing temperatures for an excitation wavelength of 255 nm

Figure 5.6 shows the fluorescence spectra of ZnO thin films annealed at different temperatures from 300-1050ºC for an excitation wavelength of 325 nm. From the figure it is clear that two emission bands are present, a UV emission band and another in the green region. The transitions from different excited states of excitons may be weakened at this higher excitation wavelength and a broad visible emission due to surface defect states become more pronounced at 325 nm excitation wavelength. The UV band has been assigned to the bandgap fluorescence and the visible band is mainly due to surface defect states.

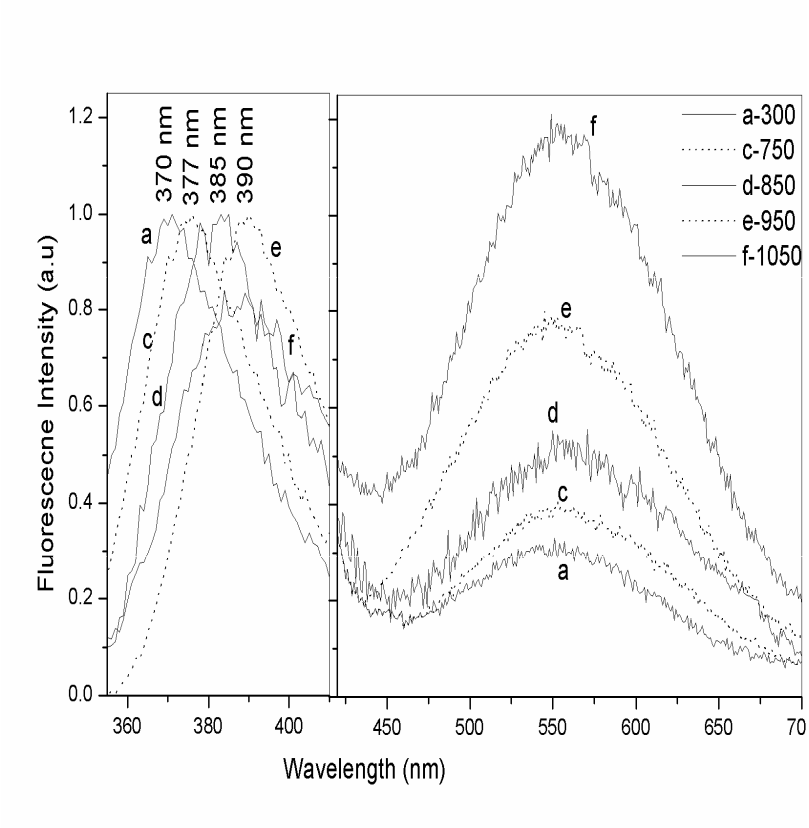

Figure 5.6: Fluorescence spectra of ZnO thin films at different annealing temperatures for an excitation wavelength of 325 nm

As the annealing temperature increases, this UV band undergoes a red shift with increase in particle size as in the case of absorption spectrum. For the intrinsic luminescence of ZnO nanoparticles, it is generally known that the formation of nanoparticles causes a red shift in the PL spectra due to quantum size effect[31]. The UV emission peak is shifted from 3.34 to 3.18 eV due to the shift of the optical bandgap from 3.44 to 3.28 eV and it clearly indicates that the origin of UV emission is the near band edge emission.

Figure 5.7(a) shows the bandgap change as a function of annealing temperature. Figure 5.7(b) shows the energy of the band to band transition as a function of the annealing temperature. Similarly figure 5.8(a) and 5.8(b) shows the bandgap change and energy of band to band transition respectively as a function of particle size.

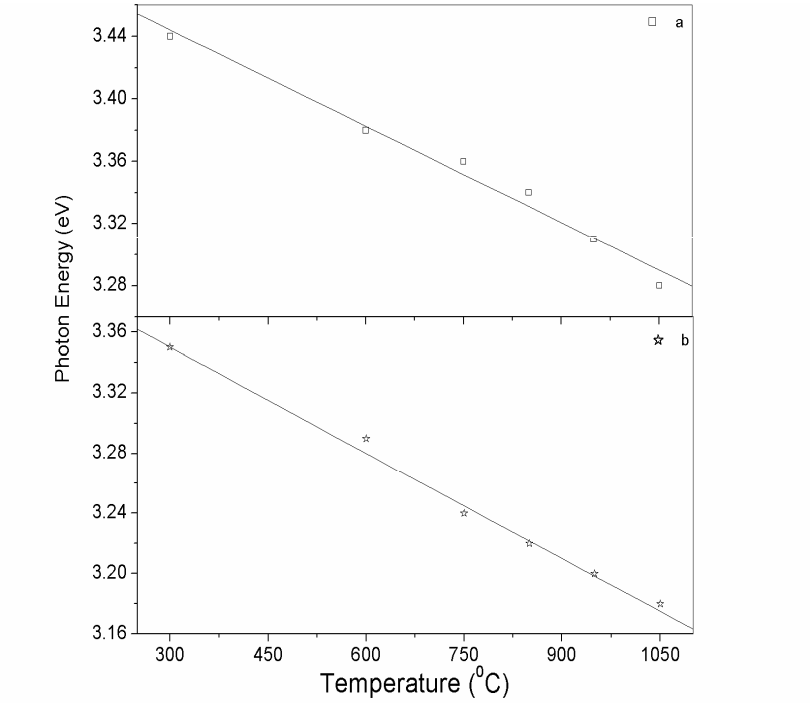

Figure 5.7:The dependence of annealing temperature on

(a) *bandgap* (b) *band to band emission*

As clearly seen in figures 5.7 and 5.8, the red shift in the UV emission with annealing temperature (particle size) closely follows the red shift in the band edge, indicating that the two are related. Mean cluster size could be principally derived from the absorption measurements and the ZnO crystallite size increases exponentially from about 4 nm to 85 nm with the rise of the annealing temperature from 300 ºC to 1050 ºC as shown in figure 5.3. This allows us to reconstruct the size distribution curves from the fluorescence spectrum.

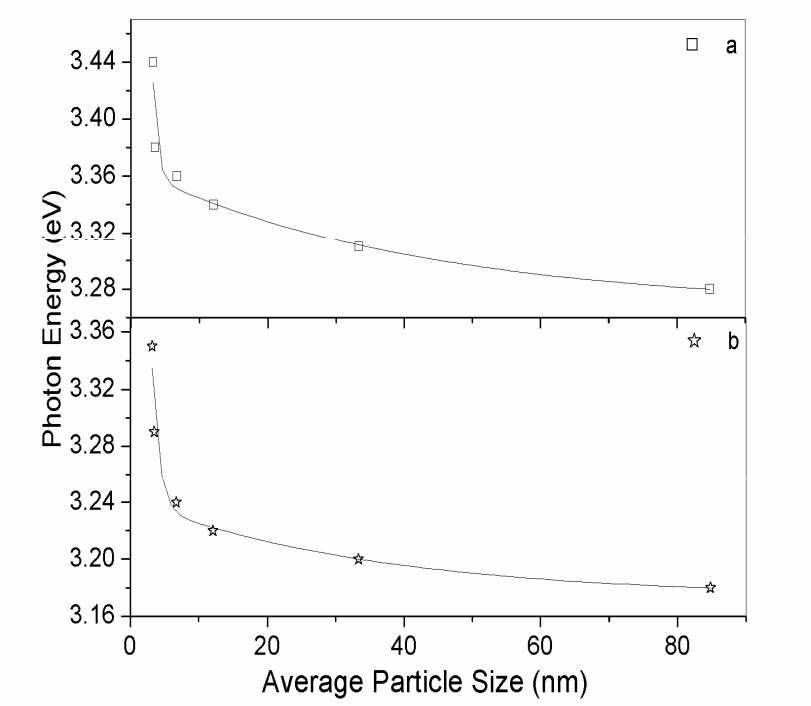

Figure 5.8:The dependence of average particle size on
(a) *bandgap* (b) *band to band emission*

The intensity of the UV emission remains the same whereas the intensity of the green emission increases with annealing temperature. However, there is a decrease in the UV luminescence intensity at an

annealing temperature of 1050^0C and this can be mainly because of the formation of interstitial vacancies when the films annealed at a high temperature.

As the annealing temperature increases, the intensity of green luminescence increases. The intensity of green emission becomes even stronger than that of UV emission at a annealing treatment of 1050°C. The intensity variation of green luminescence is systematically studied as a function of annealing temperatures in order to investigate the emission mechanism. The increase of green luminescence after annealing treatment means the increase of singly ionized oxygen vacancies according to the result of Vanheusden *et al.*[32]. Due to its *n*-type semiconductor nature, the most defects in ZnO are Zn interstitials and oxygen vacancies. The Zn interstitials in ZnO are easily ionized, and electrons produced by ionized Zn interstitials contribute to electrical conductivity and the number of Zn interstitials decreases probably due to Zn evaporation at increasing annealing temperatures[33]. However, the number of oxygen vacancies increases with increase in annealing temperature. Therefore, the intensity of green luminescence increases with increase in annealing temperature. ZnO nanopowders and thin films also show green luminescence after they were annealed in oxygen, nitrogen or air[33].

The inset of figure 5.9 shows the variation of green photoluminescence (PL) intensity depending on annealing temperature. The intensity of green emission dramatically increases above an annealing temperature of 750°C. Figure 5.9 shows a break at a transition temperature of 740^0C, suggesting a change in mechanism from a low temperature (300-650^0C) activated process to a high temperature (750-1050^0C) activated process. An indication of this change in process exists in the literature[34-35]. The practical significance of this observation is that it would now require

caution in extrapolating the high temperature data to represent behaviour in the low temperature regime.

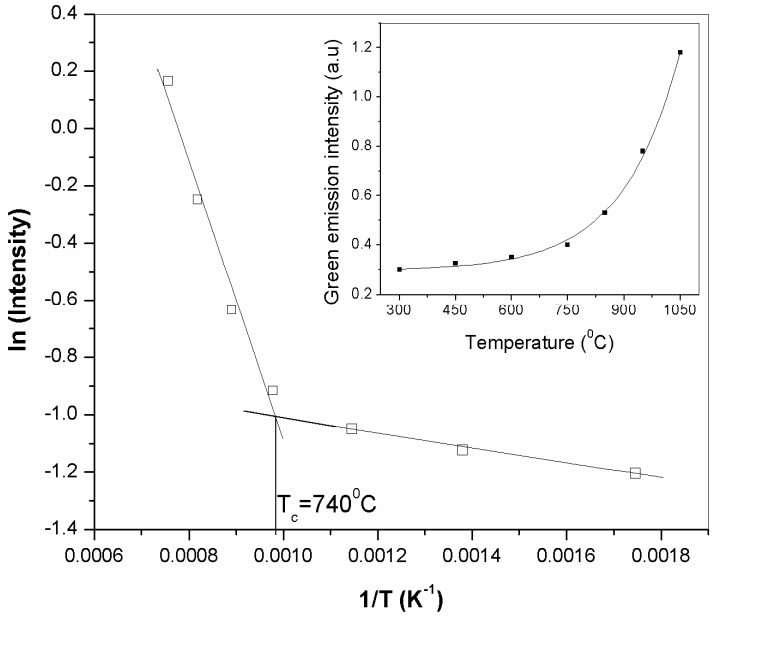

Figure 5.9: Variation of green PL intensity with annealing temperature

From these results, it is considered that many oxygen vacancies are generated due to the large lattice mismatch between the film and the substrate and provides high surface energy during the annealing process at and above the transition temperature of 740°C. Therefore the green emission related to the donor level is dominant due to the increase of oxygen vacancies (V_O^{2-}).

5.6.1 Luminescence mechanism

Figure 5.10 shows the emission mechanism of UV and visible luminescence of ZnO films. UV luminescence is caused by the transition from near conduction band edge to valence band. As temperature increases,

shift of UV luminescence is observed from 3.34 to 3.18 eV due to the shift of the optical energy gap from 3.44 to 3.28 eV. The green luminescence is mainly due to surface defect states. The UV luminescence center is not related to visible luminescence center. If green luminescence is related to the deep acceptor level, UV luminescence should have decreased as green luminescence increased. Based on these results, it can be concluded that the green luminescence of ZnO is not due to the transition from near band edge to deep acceptor level in ZnO but mainly due to the transition from deep donor level to valence band. But at 1050^0C, the UV intensity decreases. This may be attributed to the transition from near band edge to deep acceptor level due to zinc vacancies (V_{Zn}^{2+}).

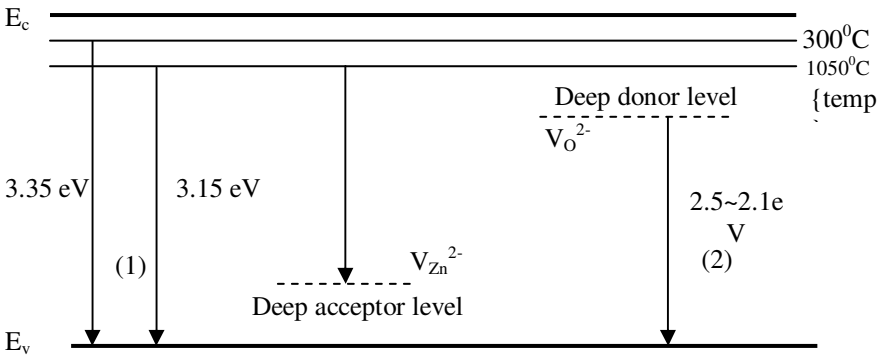

Figure 5.10:The UV and visible photoluminescence mechanism of ZnO

(1) transition from near conduction band edge to valence band

(2) transition from deep donor level to valence band

5.7 Nonlinear optical characterization

The third order nonlinear optical properties of thin films of nano ZnO are investigated using the z-scan technique and are explained in chapter 3. Film thickness is evaluated to be in the range of 60–100 nm. Figure 5.11

gives the open aperture z-scan traces of ZnO films annealed at different temperatures at a typical fluence of 300 MW/cm^2. The open aperture curve exhibits a normalized transmittance valley, indicating the presence of induced absorption in the ZnO thin films.

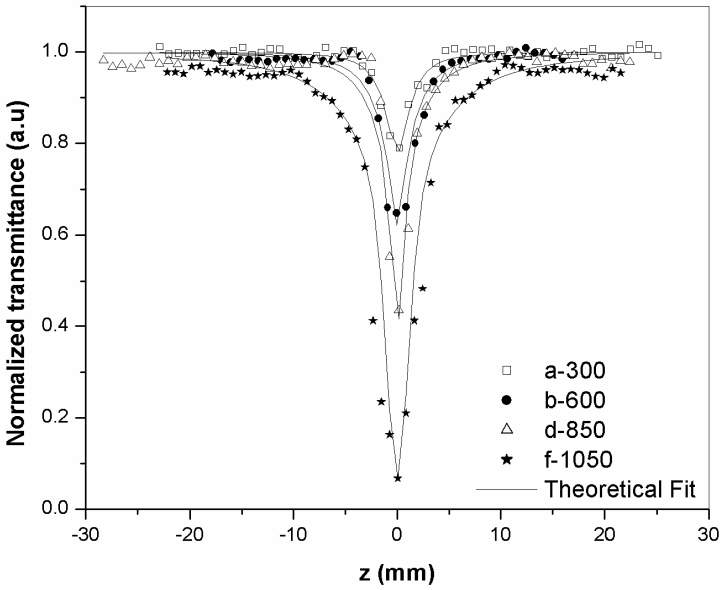

Figure 5.11: The open aperture z-scan traces of ZnO thin films at different annealing temperatures at a fluence of 300 MW/cm^2

Figure 5.12 gives the closed aperture z-scan traces of ZnO films annealed at different temperatures at a fluence of 300 MW/cm^2. The closed aperture curve exhibited a peak-to-valley shape, indicating a negative value of the nonlinear refractive index n_2. It is observed that the peak-valley of the closed-aperture z-scan satisfied the condition $\Delta z \sim 1.7\ z_0$, thus confirming the presence of cubic nonlinearity[36].

The enhancement of nonlinear optical properties with increasing dimension in accordance with increasing annealing temperature in the weak

confinement regime essentially originates from the size dependent enhancement of oscillator strength of coherently generated excitons and is explained in detail in chapter 3. The susceptibility is size dependent, without showing a saturation behavior in the size range studied in our investigation.

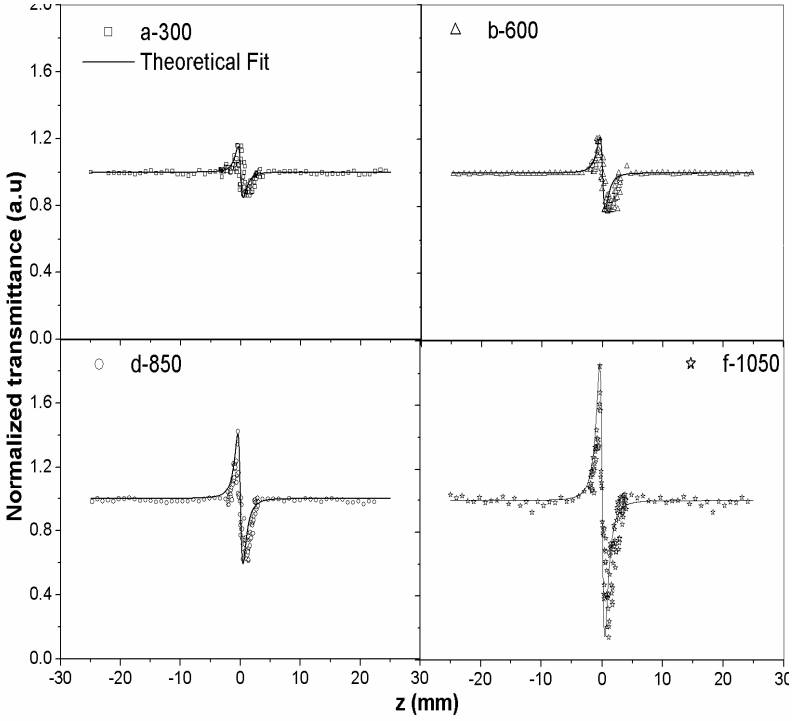

Figure 5.12: The closed aperture z-scan traces of ZnO thin films at different temperatures at a fluence of 300 MW/cm^2

The experimentally obtained values of nonlinear parameters at an intensity of 300 MW/cm^2 are shown in table 5.1. The nonlinear absorption coefficient is reported to increase from 1.2×10^{-9} m/W to 1.1×10^{-8} m/W when the annealing temperature rises from 950ºC to 1050ºC for ZnO microcrystalline films developed by sputtering technique[30]. The enhancement of nonlinear coefficients for our thin nanocrystalline films compared to microcrystalline films of ZnO is attributed to the nanosized structure of the

films since it has been reported that the reduced dimensionality of the particles resulted in considerable enhancement of the second-order susceptibility $\chi^{(2)}$ in thin films of ZnO[37]. Similar results in the third order nonlinear parameters are evident in our measurements also. Thus, the real and imaginary parts of third-order nonlinear optical susceptibility measured by the z-scan technique revealed that the ZnO thin films investigated in the present study have good nonlinear optical response and could be chosen as ideal candidates with potential applications in nonlinear optical devices.

Annealing temperature ^{0}C	β 10^{-6} m/W	n_2 10^{-5} esu	$\mathrm{Im}(\chi^{(3)})$ 10^{-6} esu	$\mathrm{Re}\,\chi^{(3)}$ 10^{-6} esu	$\lvert\chi^{(3)}\rvert$ 10^{-6} esu
300	2.9	-1.1	0.1	-2.3	2.3
600	6.9	-1.5	0.3	-3.1	3.2
750	13.8	-2.1	0.6	-4.5	4.6
850	19	-2.8	0.8	-6	6.1
950	51.8	-3.5	2.2	-7.5	7.8
1050	103.7	-5.9	4.5	-12.6	13.4

Table 5.1: Measured values of nonlinear absorption coefficient, nonlinear refractive index and third order susceptibility of ZnO thin films at an intensity of 300 MW/cm^2 for an irradiation wavelength of 532 nm at different annealing temperatures

Figure 5.13 shows the variation of $\chi^{(3)}$ as a function of annealing temperature. The data shows an exponential increase of $\chi^{(3)}$ values with increasing temperature and the values range from 2.3x10^{-6} to 1.3 x10^{-5}esu for T=300-1050ºC. For the samples annealed below 750 ºC, the absolute value

of $\chi^{(3)}$ does not change significantly, but for ones annealed above 750 ºC, the $\chi^{(3)}$ value increases rapidly with the increase of the annealing temperature. At lower temperatures and for films with small size, $\chi^{(3)}$ is small indicating that it is a third order effect[36] resulting from two photon absorption (TPA). For films of larger particle size and at higher temperatures, $\chi^{(3)}$ becomes very large indicating the occurrence of higher order nonlinear processes such as free carrier absorption. For samples annealed at higher temperatures, the $\chi^{(3)}$ value increases rapidly because of the interdiffusion of the SiO_2 substrates and ZnO films and interfacial state enhancement[30].

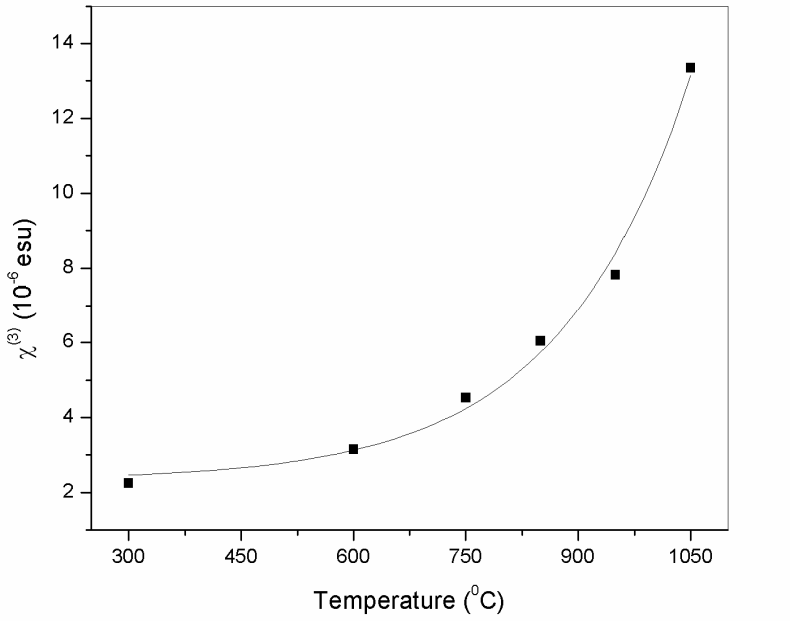

Figure 5.13: Variation of $\chi^{(3)}$ as a function of annealing temperature

For samples annealed at 1050ºC, the $\chi^{(3)}$ value is one order of magnitude larger than that at 950ºC due to the interfacial state enhancement. Furthermore, as the ZnO nanocrystallites are melted into the SiO_2 substrate, the local field effect and the interband transition of electrons from the

interfacial state to the unoccupied state near the Fermi level will greatly enhance the nonlinear absorption[38].

In order to obtain the annealing temperature and particle size dependence of the third-order susceptibility, ln (*T*) and ln (R) are plotted against ln ($\chi^{(3)}$) and are shown in figure 5.14. When we apply a least-squares fit, a temperature dependence of $T^{2.5}$ and a size dependence of R^2 is obtained indicating an enhancement of more than two orders of magnitude. From the graph, $\ln(\chi^{(3)}) \approx 2.5\ln(T)$ and $\chi^{(3)} \approx T^{2.5}$

$$\ln(\chi^{(3)}) \approx 2\ln(R) \text{ and } \chi^{(3)} \approx R^2$$

This dependence is in good agreement with that observed for CdS, CuCl and CuBr nanocrystals and ZnO colloids[39-42].

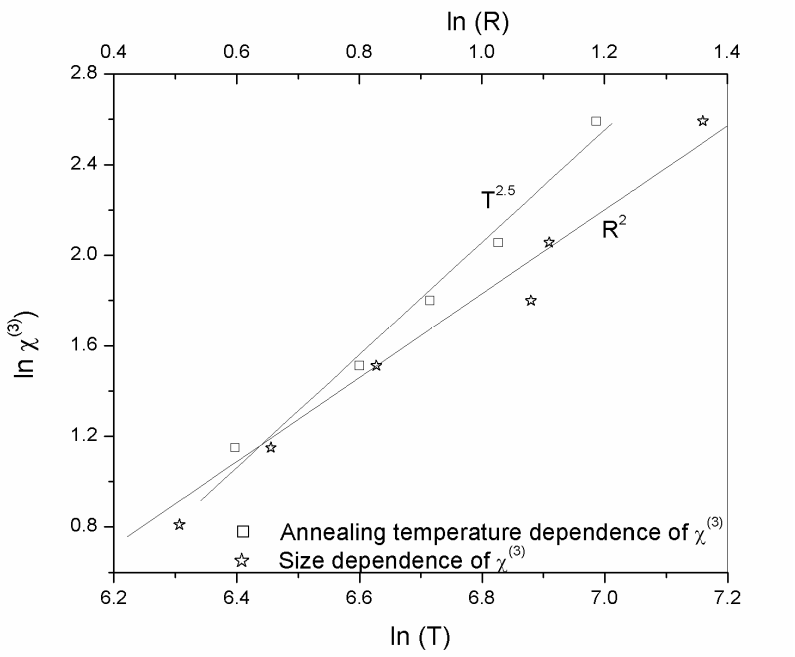

Figure 5.14: Dependence of $\chi^{(3)}$ as a function of annealing temperature and particle size for ZnO thin films. The straight lines indicate $T^{2.5}$ and R^2 dependence

5.8 Optical limiting

Optical limiters are devices that transmit light at low input fluences or intensities, but become opaque at high inputs. To examine the effect of annealing on optical limiting property of thin films of nano ZnO, the nonlinear transmission of the film is studied as a function of input fluence for different annealing temperatures. The optical limiting property occurs mostly due to absorptive nonlinearity and can be generated from z-scan traces[43]. Figure 5.15 illustrates the influence of annealing temperature on the optical limiting response.

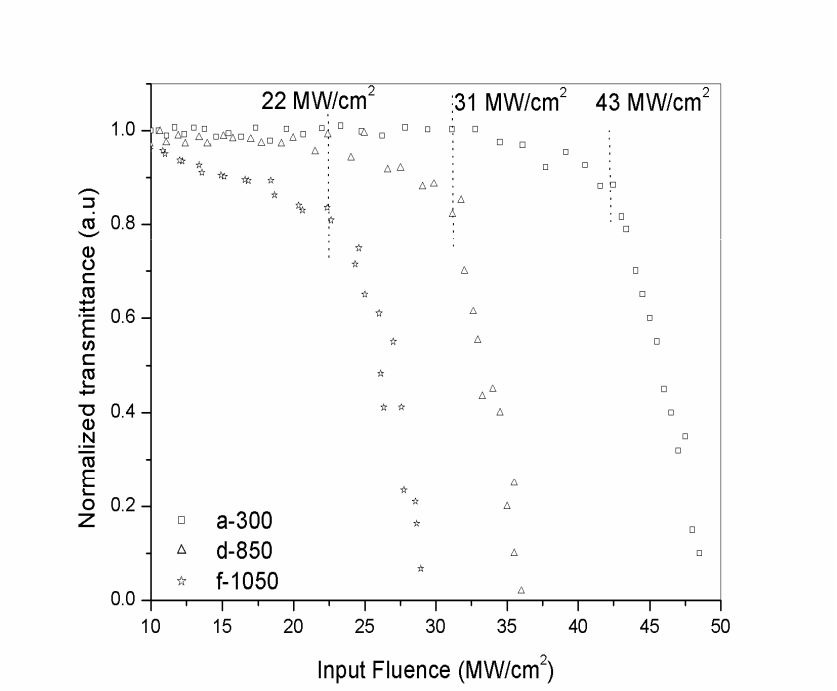

Figure 5.15: Optical limiting curves of ZnO thin films at different annealing temperatures

It is obvious that the lower the optical limiting threshold, the better the optical limiting material. The optical limiting threshold is found to be

high in the case of ZnO films annealed at a temperature of 300^0C (43 MW/cm^2) in comparison with the ZnO films annealed at a temperature of 850^0C (31 MW /cm^2) and ZnO films annealed at a temperature of 1050^0C (22 MW/cm^2). These values are comparable to the reported optical limiting threshold for ZnO nano colloids of different particle size[39, 42]. Annealing temperature and hence particle size has a significant effect on the optical limiting performance of ZnO films. Increasing the annealing temperature reduces the limiting threshold and enhances the optical limiting performance. From the measured values of β for the ZnO films, it can be seen that the film annealed at a higher temperature and having larger particle size is a better nonlinear absorber and hence a good optical limiter.

5.9 Conclusions

The annealing effect on the spectral and nonlinear optical characteristics of ZnO thin films deposited on quartz substrates by sol gel process is investigated. As the annealing temperature increases from 300-1050^0C, there is a decrease in the bandgap which indicates the changes of the interface of ZnO with substrate. Systematic studies on nano crystallites have indicated the presence of luminescence due to excitonic emissions when excited with 255 nm as well as significant contribution from surface defect states when excited with 325 nm. The intensity of UV peak remains the same while the intensity of the visible peak increases with increase in annealing temperature. The mechanism of the luminescence suggests that UV luminescence of ZnO thin films is related to the transition from conduction band edge to valence band, and green luminescence is caused by the transition from deep donor level resulting from oxygen vacancies to valence band. Nonlinear optical response of these samples is studied using nanosecond laser pulses at an off-resonance wavelength for optical limiting applications. The third order nonlinear susceptibility increases from 2.3×10^{-6} to 1.3×10^{-5}esu when the annealing temperature rises from 300ºC to 1050ºC,

mainly due to the enhancement of interfacial state and exciton oscillator strength. We have experimentally studied optical nonlinearity as a function of temperature and a $T^{2.5}$ dependence of nonlinear susceptibility is obtained for thin films of nano ZnO. Optical limiting response is temperature dependent and the film annealed at higher temperature and having larger particle size is a better nonlinear absorber and hence a good optical limiter.

5.10 References

1 W D Hunt; "*Isomorphic surface acoustic waves on multilayer structures*", J. Appl. Phys. **89**, 3245 (2001)

2 H Cao, Y G Zhao, S T Ho, E W Seelig, Q H Wang and R P H Chang, **"***Random Laser Action in Semiconductor Powder*"; Phys. Rev. Lett. **82**, 2278 (1999)

3 J G Ma, Y C Liu, R Mu, J Y Zhang, Y M Lu, D Z Shen, and X W Fan; "*Method of control of nitrogen content in ZnO films: Structure and photoluminescence properties*", J. Vac. Sci. Technol. B **22**, 94 (2004)

4 V Srikant and D R Clarke; "*Optical absorption edge of ZnO thin films: the effect of substrate*", J. Appl. Phys. **81**, 6357 (1997)

5 I Sayago, M Aleixandre, A Martinez, M J Fernandez, J P Santos, J Gutierrez, I Gracia and M C Horrillo; "*Structure studies of Zinc oxide films grown by RF magnetron sputtering*", Synth. Met. **148**, 37 (2005)

6 W L Zhang, H Wang, K S Wong, Z K Tang, G K L Wong, R Jain; "*Third-order optical nonlinearity in ZnO microcrystallite thin films*", Appl. Phys. Lett. **75**, 3321 (1999)

7 N R Aghamalyan et.al.; "*Influence of thermal annealing on optical and electrical properties of ZnO films prepared by electron beam evaporation*", Semicond. Sci. Technol. **18,** 525 (2003)

8 C L Jia, K M Wang, X L Wang, X J Zhang, F Lu; "*Formation of c-axis oriented ZnO optical waveguides by r-f magnetron sputtering*", Opt. Express **13**, 5093 (2005)

9 M K Ryu, S H Lee, M S Jang, G N Panin and T W Kang; "*Postgrowth annealing effect on structure and optical properties of ZnO films grown on GaAs substrates by the radio frequency magnetron sputtering technique*", J. Appl. Phys. **92**, 154 (2002)

10 R J Hong, J B Huang, H B He, Z X Fan and J D Shao; "*Influence of different post-treatments on the structure and optical properties of zinc oxide thin films*", Appl. Surf. Sci. **242,** 346 (2005)

11 J H Lin, Y J Chen, H Y Lin and W F Hsieh; "*Two-photon resonance assisted huge nonlinear refraction and absorption in ZnO thin films*", J. Appl. Phys. **97**, 033526 (2005)

12 V Gupta and A Mansingh; "*Influence of post-deposition annealing on the structural and optical properties of sputtered zinc oxide film*", J. Appl. Phys. **80**, 1063 (1996)

13 Y W Hong and J H Kim; "*The electrical properties of Mn3O4-doped ZnO*", Ceram. Int. **30,** 1301 (2004)

14 D H Zhang, Q P Wang and Z Y Xue; "*Photoluminescence of ZnO films excited with light of different wavelength*", Appl. Surf. Sci. **207**, 20 (2003)

15 G M Jia, G Z Zhang, W H Xiang and J B Ketterson, "*Measurement of the Third-order Nonlinear Optical Coefficient of ZnO Crystals by Using ICCD-Z-Scan*", Chin. Phys. Lett. **21**, 1356 (2004)

16 X J Zhang, W Ji and S H Tang; "*Determination of optical nonlinearities and carrier lifetime in ZnO*", JOSAB **14**, 1951 (1997)

17 X Zhang, H Fang, S Tang, W Ji, "*Determination of two-photon-generated free-carrier lifetime in semiconductors by Z-scan technique*", Appl. Phys. B **65**, 549 (1997)

18 S S Lin, J L Huang and D F Liil; "*Effect of substrate temperature on the properties of Ti-doped ZnO films by simultaneous rf and dc magnetron sputtering*", Mater. Chem. Phys. **90**, 22 (2005)

19 X H Yu, J Ma, F Ji, Y H Wang, X J Zhang, C F Cheng and H L Ma; "*Effects of sputtering power on the properties of ZnO:Ga films deposited by r. f. magnetron-sputtering at low temperature*", J. Cryst. Growth **274**, 474 (2005)

20 R J Hong, H J Qi, J B Huang, H B He, Z X Fan and J D Shao; Thin Solid Films **473**, 58 (2005)

21 Z B Fang, Z J Yan, Y S Tan, X Q Liu and Y Y Wang; "*Influence of post-annealing treatment on the structure properties of ZnO films*", Appl. Surf. Sci. **241**, 303 (2005)

22 http/hyperphysics.phy-astr.gsu.edu/hbase/hframe.html

23 Joachin Piprek; "*Semiconductor optoelectronic devices: Introduction to physics and simulation*", Academic press, Elsevier -USA (2003)

24 R Passler; Phy. Stat. Solidi (b) **216**, 975 (1999)

25 Y P Varshni; "*Temperature dependence of the energy gap in semiconductors*" Physica **34**, 149 (1967)

26 C Jagadish and S J Pearton; "*ZnO: bulk, thin films and nanostructures: Processing, properties and applications*" Elsevier (2006)

27 D Luna-Moreno, E De la Rosa-Cruz, F J Cuevas, L E Regalado, P Salas, R Rodríguez and V M Castano; "*Refractive index measurement of pure and Er^{3+}-doped ZrO_2–SiO_2 sol–gel film by using the Brewster angle technique* ", *Opt. Mat.*, **19**, 275 (2002)

28 V Kumar and B S R Sastry; "*Thermal expansion coefficient of binary semiconductors*", Cryst. Res. Technol. **36** (6), 565 (2001)

29 H L Cao, X F Qian, Q Gong, W M Du, X D Ma and Z K Zhu; "*Shape- and size-controlled synthesis of nanometre ZnO from a simple solution route at room*

temperature", Nanotechnology **17,** 3632 (2006)

30 Y B Han, J B Han, S Ding, D J Chen and Q Q Wang "*Optical nonlinearity of ZnO microcrystallite enhanced by interfacial state*", Opt. Express, **13** (23), 9211 (2005)

31 Litty Irimpan, A Deepthy, Bindu Krishnan, V P N Nampoori and P Radhakrishnan, J. Appl. Phys. **102**, 063524 (2007)

32 K. Vanheusden, W. L. Warren, C. H. Seager, D. R. Tallant, J. A. Voigt, and B. E. Gnade; "*Mechanisms behind green photoluminescence in ZnO phosphor powders*", J. Appl. Phys., **79**, 7983 (1996)

33 J.Z. Wang, G.T. Du, Y.T. Zhang, B.J. Zhao, X.T. Yang, D.L. Liu; "*Luminescence properties of ZnO films annealed in growth ambient and oxygen* ", J. Crystal Growth., **263**, 269 (2004)

34 T K Gupta,W D Straub; "*Effect of annealing on the ac leakage components of the ZnO varistor. I. Resistive current*" J. Appl. Phys. **68**, 845 (1990)

35 V Gavryushin, G Raciukaitis, D Judozbalis, A Kazlauskas and V Kubertavicius; "*Characterization of intrinsic and impurity deep levels in ZnSe and ZnO crystals by nonlinear spectroscopy*" J. Cryst. Growth, **138**, 924 (1994)

36 M S Bahae, A A Said and E W van Stryland; "*High-sensitivity, single-beam n_2 measurements"*, *Opt Lett*, **14**, 955 (1989)

37 Gang Wang, G. T. Kiehne, G. K. L. Wong, J. B. Ketterson, X. Liu, and R. P. H. Chang; "*Large second harmonic response in ZnO thin films*", Appl. Phys. Lett. **80**, 401, (2002)

38 R. G. Xie, J. Q. Zhuang, L. L. Wang, W. S. Yang, D. J. Wang, T. J. Li and J. N. Yao, "A WO3/ZnO nanoparticle composite system with high photochromic performance," Chem. J. Chinese U. **24**, 2086 (2003)

39 W Jia, E P Douglas, Fenggi Guo and Wenfang Suna; "*Optical limiting of semiconductor nanoparticles for nanosecond laser pulses*", Appl. Phys. Lett. **85** (26), 6326 (2004)

40 Takumi Kataoka, Takashi Tokizaki and Arao Nakamura, "*Mesoscopic enhancement of optical nonlinearity in CuCl quantum dots: Giant-oscillator strength effect on confined excitons*", Physical Review B, **48**, 2815 (1993)

41 Yingli Li, Masaki Takata and Arao Nakamura; "*Size-dependent enhancement of nonlinear optical susceptibilities due to confined excitons in CuBr nanocrystals*", *Physical Review B*, **57**,15 (1998)

42 Litty Irimpan, Bindu Krishnan, A Deepthy, V P N Nampoori and P Radhakrishnan; Journal of applied physics **103**, 033105 (2008)

43 F. M. Quereshi, S.J. Martin, X. Long, D.D.C. Bradley, F.Z. Heneri, W.J. Balu, E.C. Smith, C.H. Wang, A.K. Kar and H.L. Anderson; "*Optical limiting properties of a zinc porphyrin polymer and its dimer and monomer model compounds* ", *Chem. Phys*., **231**, 87 (1998)